

# High Performance Organic Thin-Film Transistor based on Amorphous A, B-Alternating Poly(arylenevinylene) Copolymers

Tae-Lim Choi,<sup>\*,†,‡</sup> Kuk-Min Han,<sup>§</sup> Jeong-Il Park,<sup>§</sup> Do Hwan Kim,<sup>§</sup> Jun-Mo Park,<sup>†</sup> and Sangyoon Lee<sup>\*,§</sup>

<sup>†</sup>Department of Chemistry, College of Natural Sciences, Seoul National University, Seoul 151-747, South Korea, <sup>‡</sup>Advanced Material Group, Electronic Chemical Materials R&D Center, Cheil Industries Inc., 332-2 Gocheon-dong, Uiwang-si, Gyunggi-do 437-711, South Korea, and <sup>§</sup>Display Lab, Material and Device Institute, Samsung Advanced Institute of Technology, Samsung Electronics Co., Ltd., Mt. 14-1, Nongseo-dong, Giheung-gu, Yongin-si, Gyeonggi-do 446-712, South Korea

Received May 13, 2010; Revised Manuscript Received June 8, 2010

**ABSTRACT:** A series of amorphous polymers of poly(arylenevinylene) copolymers, in which heterocycles (furan, thiophene, selenophene) and dialkoxy phenylenes were alternately linked by vinylene unit, was prepared by the Horner–Emmons reaction. Because of high regularity of the polymer microstructure by selective formation of *E* olefin, the resulting polymers showed good interchain  $\pi$ – $\pi$  stacking in thin film state despite being amorphous polymers. When the A,B-alternating poly(phenylene thiophene vinylene), in particular with the bis(heptoxy) group, was used as a semiconductor material in an organic thin-film transistor, the best hole mobility up to 0.03 cm<sup>2</sup>/(V s) was observed, which is one of the highest values recorded from amorphous polymer film. The mobility was even improved to 0.06 cm<sup>2</sup>/(V s) when the polymer was blended with well-dispersed single-wall carbon nanotubes (SWCNT). Although this mobility is lower than that from the best crystalline polymers, these amorphous polymers showed advantages such as the device performances being less sensitive to both their molecular weights and the choice of gate insulators than the typical crystalline polymers.

## Introduction

Extensive research on organic thin-film transistors (OTFT) has been carried out during past decade.<sup>1</sup> Especially, soluble materials made of oligomers and polymers are attractive because they allow for room temperature solution fabrication such as spin coating and inkjetting printing. As a result, large-area displays at much lower cost can be manufactured and ultimately, these materials are expected to be the key for the manufacturing of the flexible electronic devices.<sup>2</sup> For these reasons, the polymeric semiconductors gained attractions even though the devices made of vacuum deposited small molecules performed much better as a transistor.<sup>3</sup> Among the various polymeric semiconductors reported, polymers that give good OTFT performance are crystalline polymers such as poly(3-hexylthiophene) (P3HT)<sup>4</sup> and liquid-crystalline polymers such as poly(9,9'-*n*-dioctylfluorene-*alt*-bithiophene) (F8T2),<sup>5</sup> poly(3,3'-didodecyl quaterthiophene) (PQT-12)<sup>6</sup> and particularly poly(2,5-bis(3-dodecylthiophene-2-yl)thieno[3,2-*b*]thiophene) (PBTTT), whose OTFT performance is as good as commercialized amorphous silicon transistors.<sup>7</sup>

On the other hand, amorphous polymers received little attention due to its intrinsically poor OTFT performances arising from slower charge transport due to the lower degree of molecular ordering leading to the slower hopping process. However, amorphous polymers can be beneficial as they provide uniform film morphology which improves the reproducibility of the device performance during the device manufacturing. Also, the manufacturing process can be simplified because device performances using amorphous materials can be less sensitive to device fabrication conditions compared to device using crystalline materials. Recently, good TFT performance was demonstrated when

amorphous polymers such as poly(triarylamine)s (PTAA),<sup>8</sup> poly(phenylene vinylene) (PPV),<sup>9</sup> and fluorene-containing polymers<sup>10</sup> were used as channel materials in OTFT devices. Herein, we report the synthesis of amorphous phenylene arylene vinylene copolymers where electron rich heteroatom such as sulfur and selenium are incorporated into the polymer backbone to improve the hole mobility for OTFT devices. Also to compensate the lack of crystallinity, the region-regular A,B-alternating copolymer microstructure was chosen to enhance the intermolecular packing. As a result, we demonstrate that various amorphous A,B-alternating copolymers can be used to give high performance OTFTs with hole mobility up to 0.03 cm<sup>2</sup>/(V s).

## Results and Discussion

Our concept of polymer design starts from simple ideas that symmetric phenylene monomer unit with linear dialkoxy chains would provide the solubility for the whole polymer and reasonable molecular packing. Furthermore, aryls of electron rich heterocycles may increase hole transport. Finally these two monomer units should be alternately linked by vinylene group to give planarity to the polymer backbone leading to better  $\pi$ – $\pi$  stacking. To maximize the stereoregularity and regioregularity of newly formed vinylene groups, the Horner–Emmons reaction was chosen over Gilch, Heck, or Wittig reactions to produce A,B-alternating copolymers with excellent *E* olefin stereochemistry.<sup>11</sup> On the basis of these criteria, various A,B-alternating copolymers were synthesized from the heteroatoms containing dialdehyde monomers **1** such as 2,5-thiophenedicarboxaldehyde and its selenophene and furan derivatives and monomer **2**, phenylene units with varying lengths of alkoxy chains. (Scheme 1)

A typical Horner–Emmons polymerization was carried out by slow addition of 3 equiv of base, 1 M KO<sup>t</sup>Bu in THF to the

\*Corresponding authors. E-mail: (T.-L.C.) tlc@snu.ac.kr; (S.L.) sangyoon.lee@samsung.com.

Scheme 1. Synthesis of Poly(arylenevinylene)

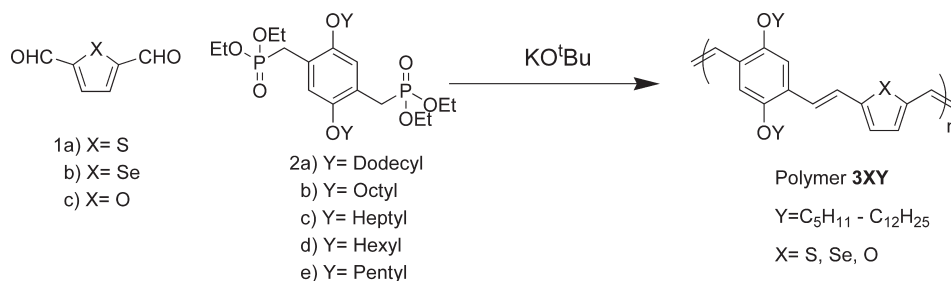


Table 1. Chemical and Electronic Properties of the Polymers

polymer	$M_n$ (kg/mol) <sup>a</sup>	$E_g$ (eV) <sup>b</sup>	$\mu$ (cm <sup>2</sup> /(V s)) <sup>c</sup>	on-off ratio
3aa	21	2.0	0.001	10 <sup>4</sup>
3ab	16	2.0	0.014	10 <sup>5</sup>
3ac	62	2.0	0.022	10 <sup>5</sup>
3ad	55	2.0	0.013	5 × 10 <sup>4</sup>
3ae	15	1.9	0.007	5 × 10 <sup>4</sup>
3bb	14	1.9	0.013	10 <sup>4</sup>
3bc	10	1.9	0.011	10 <sup>4</sup>
3bd	16	1.9	0.008	5 × 10 <sup>5</sup>
3cd	22	2.0	0.003	10 <sup>3</sup>
3ce	13	2.0	0.002	10 <sup>3</sup>

<sup>a</sup>  $M_n$  measured by size exclusion chromatography relative to polystyrene standards with THF elutant. <sup>b</sup>  $E_g$  measured by UV-vis spectra from the offset. <sup>c</sup> OTFT device geometry: top-contact, W/L = 1000 μm/100 μm. Source/drain: Au, measured in air.

monomer solution in THF and it was refluxed for 12 h. Then the polymerization was quenched by acidic work-up and poured into excess methanol and subsequently into acetone to give reddish orange solid in 50 to 80% isolated yield. The resulting polymers were readily soluble in common organic solvents such as chloroform, toluene, THF, and chlorobenzene. Molecular weights for these polymers were measured by size exclusion chromatography (SEC) relative to polystyrene standards eluted by THF. Polymers had  $M_n$  in the range from 10 to 60 kg/mol with polydispersity index (PDI) greater than 2 as outlined in Table 1. <sup>1</sup>H NMR indeed revealed that the stereoregularity for the polymers prepared from Horner–Emmons reaction was excellent (See Figure SI-1 in the Supporting Information).

To examine the morphology of the polymers, dynamic scanning calorimetry (DSC) analysis was conducted and showed no endothermic or exothermic peaks during the second heating and cooling cycle for these polymers implying amorphous nature of the polymers. To further support this, the polymer films annealed at various temperatures from room temperature to above 200 °C were subjected to X-ray diffraction (XRD), and all showed no distinct pattern confirming the amorphous morphology (Figure 1).

To get more insights into the electro-chemical properties of the polymers prepared, highest occupied molecular orbital (HOMO) energy levels were measured by photoelectron spectroscopy (PES). These polymers were found to have deep HOMO levels mostly in the range of −5.4 to −5.6 eV which are larger than those of polythiophene derivatives, but similar to that of MEH-PPV. This may provide good chemical stability against air oxidation doping and increase the device lifetime. Also their band gap energies ( $E_g$ ) were obtained from the onset of the low energy optical absorption peak edges of UV-vis absorption spectra and found to be between 1.9 and 2.0 eV. (Table 1) General trends were noticed as the  $E_g$ s of the polymers decreased slightly with shorter chain length and selenium containing polymers also had slightly smaller values than those with thiophene or furan moiety. Smaller  $E_g$ s for selenophene containing polymers was due to its richer electron density compared to thiophene and furan derivatives.<sup>11a</sup>

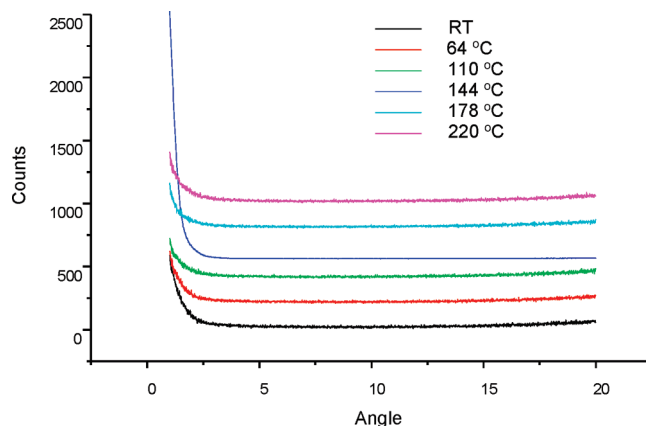
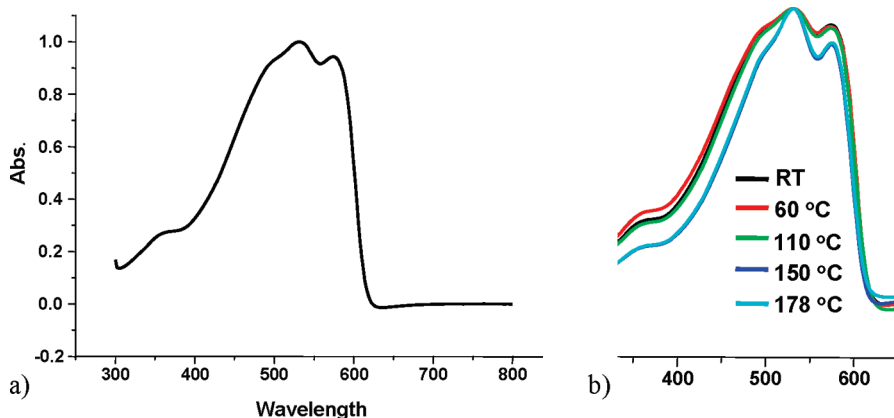


Figure 1. XRD data obtained from polymer 3ac at various temperatures.

Interestingly, Kubo and the co-workers prepared similar polymers via Wittig reaction and reported  $E_g$ s of 2.4 eV for thiophene containing polymer and 2.3 eV for that of selenophene, whose values are significantly larger than the values from our results.<sup>11a</sup> Wittig reaction produces mixture of stereoisomers, *E* and *Z* olefins whereas the Horner–Emmons reaction exclusively produces *E* olefins, resulting in excellent stereoregularity.<sup>12</sup> Thus, this comparison shows that the stereoregular polymers prepared by the Horner–Emmons method have longer conjugation length leading to lower band gap polymers.

Although the polymers are amorphous in nature, one can clearly observe the strong shoulder peaks from UV-vis spectra of the film polymer of 3ac implying good  $\pi$ – $\pi$  stacking between polymer chains. (Figure 2) The large shoulders were also observed for the other thiophene and selenophene containing polymers but the shoulders are greatly reduced for the polymers furan. Notably, this large shoulder is absent for the previously reported polymer with the same backbone unit but with branched 2-methoxy-5-(2'-ethylhexyloxy) side chain.<sup>13</sup> This major difference is due to the bulky branches disrupting the  $\pi$ – $\pi$  stacking whereas our polymers with linear and symmetric alkoxy chains enhanced  $\pi$ – $\pi$  stacking. Even more surprising is that the UV-vis spectra of the same polymer prepared by Heck reaction do not show the shoulder peaks either because Heck reaction also produces other isomers lowering the stereoregularity.<sup>11b</sup> This marked difference is again due to the difference in polymerization method where the Horner–Emmons reaction exclusively produces *E*-isomer olefins whereas Wittig and Heck reactions produce polymers with lower regioregularity.<sup>14</sup> These observations strongly suggest that the polymers with excellent stereoselectivity result in longer conjugation length and better  $\pi$ – $\pi$  stacking, and this regularity should be in great favor for the better charge transport mobility.

Notably, when the UV spectra of the polymers in solution were measured, the shoulder peak disappears as expected, and the differences between  $\lambda_{\max}$  in solution and that in the thin film was



**Figure 2.** UV-vis spectrum of the thin film polymer (a) **3ac** on quartz and (b) that when annealed at different temperatures.

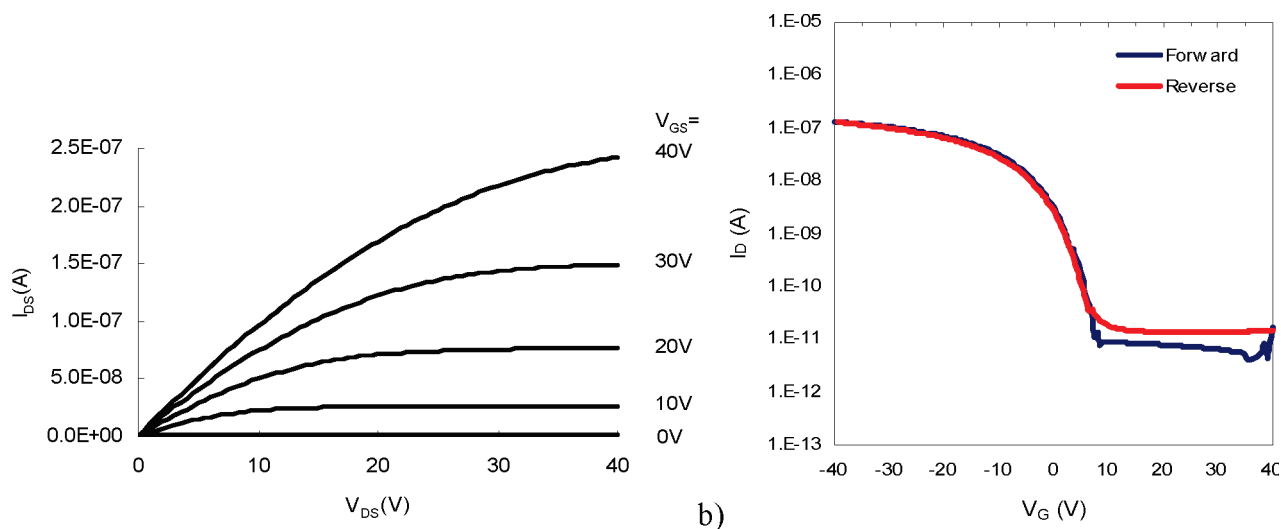


**Figure 3.** (a) Output curve and (b) transfer curve at  $V_{ds} = 10$  V for the device fabricated by polymer **3ac**.

relatively small (ca. 20 nm) compared to the difference of the crystalline polymers such as regioregular P3HT (100 nm),<sup>15</sup> and PQT-12 (75 nm),<sup>5</sup> but similar to that of amorphous regiorandom P3HT and other reported amorphous polymer.<sup>10</sup> It seems that although  $\pi$ - $\pi$  stacking appears to be substantial, the degree of ordering in the solid state is poor due to the amorphous morphology.

To our surprise, these polymers were found to be stable even at high temperatures as thermogravimetric analysis (TGA) revealed that they were found to be stable with no loss of mass up to 300 °C. Particularly, when UV-vis spectra were measured for the film annealed at various temperatures from room temperature to 180 °C, almost no reduction in  $\lambda_{max}$  was observed and the shoulder peaks were maintained at 180 °C. (Figure 2b) This implies that the conjugation length and the degree of  $\pi$ - $\pi$  stacking are retained at these temperatures.

With the polymers' characterization in hand, their TFT performances were screened. To make the devices with the top-contact geometry, 1 wt % polymer solutions in chlorobenzene was spin-coated onto the silicon-based organic insulating layer,<sup>16</sup> and gold was deposited on top of the polymer film as source and drain electrodes. First, poly(phenylene-thiophene-vinylene) series were evaluated and found that the device made from polymer **3aa** with dodecyl side-chain gave field-effect mobility of 0.001 cm<sup>2</sup>/(V s). Fortunately reducing the chain length to octyl group, **3ab**, resulted in a 10-fold increase in mobility (0.01 cm<sup>2</sup>/(V s)), and the max mobility of 0.022 cm<sup>2</sup>/(V s) with on/off ratio of 10<sup>5</sup> was

obtained with heptyl group, **3ac**. (Figure 3) No further improvement in TFT performance was noticed with even shorter alkoxy chains, **3ad** and **3ae**, hexyl and pentyl groups, respectively. It seems the poorer solubility becomes the issue for hexyl and pentyl groups. Then the devices were prepared from the more electron-rich selenophene analogues (**3bb**–**3bd**) expecting the better TFT performances. Although they had lower band-gaps than thiophene derivatives by 0.1 eV, their performances are similar or lower than those of thiophene analogues with mobilities approximately 0.01 cm<sup>2</sup>/(V s). One can suspect the larger size of selenium atom that compensated the lower band gap effect. (Table 1) Polymers of furanyl derivatives showed inferior field-effect mobilities, an order of magnitude lower than thiophene and selenophene analogues as one might expect from their poor  $\pi$ - $\pi$  stacking observed in UV spectra. Generally, the maximum hole mobilities for this family of polymers were obtained when the polymer film was annealed at 70 °C.

To investigate how TFT performances vary on different surface, two other surfaces, bare SiO<sub>2</sub> and that modified with crystalline octadecyltrichlorosilane (ODTS),<sup>17</sup> were used to fabricate the devices with the best polymer, **3ac**. As expected, using the different gate insulators resulted in different FET performances. The device made from the bare SiO<sub>2</sub> as gate insulator (GI) gave lower mobility of 0.005 cm<sup>2</sup>/(V s) whereas that from highly hydrophobic ODTS treated surface gave slightly higher mobility up to 0.03 cm<sup>2</sup>/(V s) which is one of the best values for the OTFT devices made from amorphous polymers. The difference between the worst and the

Scheme 2. Synthesis of the Similar Polymer, 4, Ether Linkage

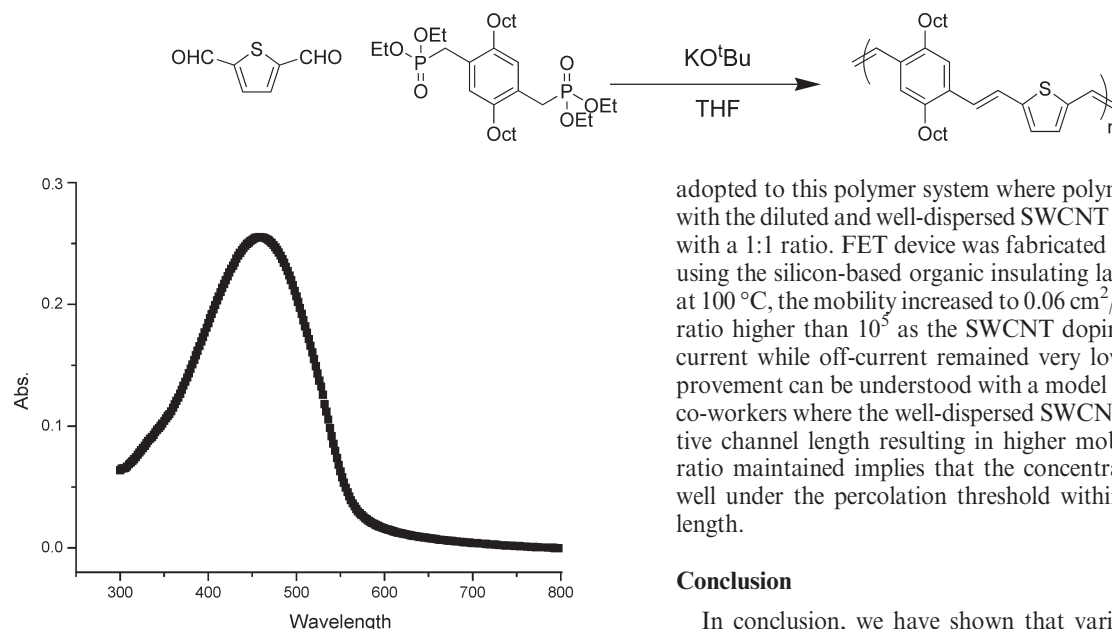


Figure 4. UV-vis spectrum of the thin film obtained from polymer 4.

best GI was less than 1 order of magnitude which is relatively small compared to the typical crystalline polymers. This suggests that the overall morphology of the amorphous film is not that sensitive to the surface property of GI.

Then molecular weight (MW) dependency on mobility was also investigated. Three samples of **3ad** with three different molecular weights (14K, 28K, and 55K) with similar PDIs (2.8, 3.0, and 3.1, respectively) were fabricated into the TFT devices and under the same condition, all showed similar mobilities, 0.011, 0.011, and 0.013 cm<sup>2</sup>/(V s), respectively, despite the large MW difference. This is again sharp contrast to the crystalline polymers where orders of magnitude deviation in the mobility may occur from the same samples with different MW.<sup>18</sup> This interesting observation can be attributed to the nature of amorphous polymers having much less significance of MW affecting the morphology change whereas the film morphology for the crystalline polymers varies greatly depending on their MW. Therefore, amorphous polymers have advantages since the film quality is well-controlled regardless of the MW and the cell to cell deviation may appear to be smaller compared to the crystalline polymers.

Interestingly, a small change in polymer backbone resulted in a subtle change in the molecular packing and the hole mobility. Instead of bis-alkoxy side chain, the same thiophene monomer was polymerized with bis-octyl phenylene derivative by the same procedure. (Scheme 2) The resulting polymer **4** just lacking the oxygen in the phenyl ring, gave no shoulder from the film UV-vis spectrum implying very little  $\pi$ - $\pi$  stacking. (Figure 4) This, in turn, is manifested onto OTFT performance as the device showed 2 orders of magnitude lower mobility (10<sup>-4</sup> cm<sup>2</sup>/(V s)) than that of **3ab** (-OC<sub>8</sub>H<sub>17</sub>) when fabricated by the same method. This large difference in the mobility can be attributed to the superior  $\pi$ - $\pi$  overlap between alkoxy polymers due to their smaller size (-O- vs -CH<sub>2</sub>-) and the more electron-rich polymer backbone. This result is significant as it reminds us that the fine-tuning of the structures and functional groups in polymer design is crucial.

Recently, scientists from Toray Industries reported the mobility enhancement by adding small amount of well-dispersed single-wall carbon nanotube (SWCNT).<sup>19</sup> This strategy was

adopted to this polymer system where polymer **3ac** was blended with the diluted and well-dispersed SWCNT solution from Toray with a 1:1 ratio. FET device was fabricated by the same method using the silicon-based organic insulating layer. After annealing at 100 °C, the mobility increased to 0.06 cm<sup>2</sup>/(V s) with the on/off ratio higher than 10<sup>5</sup> as the SWCNT doping increased the on-current while off-current remained very low. This marked improvement can be understood with a model proposed by Bo and co-workers where the well-dispersed SWCNT film reduces effective channel length resulting in higher mobility.<sup>20</sup> High on/off ratio maintained implies that the concentration of SWCNT is well under the percolation threshold within the given channel length.

## Conclusion

In conclusion, we have shown that various A,B-alternating copolymers could be prepared by the Horner-Emmons reaction between bis(alkoxy)-substituted phenylene diphosphonates and dicarboxylaldehydes of heterocycles. Although these polymers exhibited amorphous morphology, they showed good  $\pi$ - $\pi$  stacking. Their good  $\pi$ - $\pi$  stacking was attributed to the result of constructing highly stereoregular vinylene backbone repeat unit with excellent *E* selectivity via the Horner-Emmons reaction. Therefore, the OTFT devices fabricated by these polymers showed good mobilities up to 0.03 cm<sup>2</sup>/(V s), one of the best performances for amorphous polymers. A small dependency of polymer MW on OTFT device performances was observed, and the choice of insulator affected the device performance to some degree but not as much as the other reported crystalline polymers. These two factors demonstrate the benefit of using amorphous polymers. However, the choice of the side chain was critical as the mobility can defer greatly (more than 2 orders of magnitude) even with the seemingly small changes in the side chains such as replacing oxygen with a methylene unit. Lastly, we find that CNT doping significantly enhances the performance up to 0.06 cm<sup>2</sup>/(V s).

## Experimental Section

Anhydrous solvents, 2,5-thiophenedicarboxaldehyde, 2,5-furandicarboxaldehyde, and 1 M potassium *tert*-butoxide in THF were purchased from Aldrich and TCI (2,5-furandicarboxaldehyde). 2,5-Selenophenedicarboxaldehyde<sup>8a</sup> and 1,4-bis(diethylphosphonate methyl)-2,5-dialkoxybenzene were prepared by known methods.<sup>10b</sup> <sup>1</sup>H NMR spectra, IR spectra, and UV-vis spectra were measured with a Bruker NMR 300 MHz (DPX 300) spectrometer, FT-IR (EXCALIBUR) spectrometer and a Shimadzu UV-3100 spectrometer, respectively. XRD patterns were recorded on a Philips XPERT diffractometer. HOMO levels were measured by photoelectron spectroscopy in the air (PESA, model AC-2, Riken Keiki Co., Ltd.). SEC analysis was performed with a liquid chromatography system with a PL Gel Mixed Column using THF as an eluent.

**General Polymerization.** All polymers were prepared by following a typical Horner-Emmons reaction procedure. To a flask charged with two monomers in THF solution, 1 M *t*-BuOK solution in THF was added dropwise. The reaction was refluxed for 12 h under nitrogen atmosphere. The polymerization was quenched by the addition of aqueous ammonium chloride. After aqueous work-up, the polymer solution was precipitated into excess methanol, followed by the second precipitation into



excess acetone. The isolated yields are generally 50–80% after two precipitation steps.

Polymer **3aa**:  $M_n = 21\,000$  g/mol (SEC); PDI = 3.0.  $^1\text{H}$  NMR (300 MHz,  $\text{CDCl}_3$ ),  $\delta$  (ppm): 7.2–7.3 (m, 4H), 7.0 (s, 2H), 6.9 (s, 2H), 4.0 (t, 4H), 1.9 (t, 4H), 1.6 (m, 4H), 1.2–1.4 (br, 32H), 0.9 (t, 6H).

Polymer **3ab**:  $M_n = 16\,000$  g/mol (SEC); PDI = 3.0.  $^1\text{H}$  NMR (300 MHz,  $\text{CDCl}_3$ ),  $\delta$  (ppm): 7.2–7.3 (m, 4H), 7.0 (s, 2H), 6.9 (s, 2H), 4.0 (t, 4H), 1.9 (t, 4H), 1.6 (m, 4H), 1.2–1.4 (br, 16H), 0.9 (t, 6H).

Polymer **3ac**:  $M_n = 62\,000$  g/mol (SEC); PDI = 3.0.  $^1\text{H}$  NMR (300 MHz,  $\text{CDCl}_3$ ),  $\delta$  (ppm): 7.2–7.3 (m, 4H), 7.0 (s, 2H), 6.9 (s, 2H), 4.0 (t, 4H), 1.9 (t, 4H), 1.6 (m, 4H), 1.2–1.4 (br, 12H), 0.9 (t, 6H).

Polymer **3ad**:  $M_n = 55\,000$  g/mol (SEC); PDI = 3.0.  $^1\text{H}$  NMR (300 MHz,  $\text{CDCl}_3$ ),  $\delta$  (ppm): 7.2–7.3 (m, 4H), 7.0 (s, 2H), 6.9 (s, 2H), 4.0 (t, 4H), 1.9 (t, 4H), 1.6 (m, 4H), 1.2–1.4 (br, 8H), 0.9 (t, 6H).

Polymer **3ae**:  $M_n = 15\,000$  g/mol (SEC); PDI = 3.2.  $^1\text{H}$  NMR (300 MHz,  $\text{CDCl}_3$ ),  $\delta$  (ppm): 7.2–7.3 (m, 4H), 7.0 (s, 2H), 6.9 (s, 2H), 4.0 (t, 4H), 1.9 (t, 4H), 1.6 (m, 4H), 1.2–1.4 (br, 4H), 0.9 (t, 6H).

Polymer **3bb**:  $M_n = 14\,000$  g/mol (SEC); PDI = 2.9.  $^1\text{H}$  NMR (300 MHz,  $\text{CDCl}_3$ ),  $\delta$  (ppm): 7.3 (d, 2H), 7.2 (d, 2H), 7.1 (s, 2H), 7.0 (s, 2H), 4.0 (t, 4H), 1.9 (t, 4H), 1.6 (m, 4H), 1.3–1.4 (br, 16H), 0.9 (t, 6H).

Polymer **3bc**:  $M_n = 10\,000$  g/mol (SEC); PDI = 2.5.  $^1\text{H}$  NMR (300 MHz,  $\text{CDCl}_3$ ),  $\delta$  (ppm): 7.3 (d, 2H), 7.2 (d, 2H), 7.1 (s, 2H), 7.0 (s, 2H), 4.0 (t, 4H), 1.9 (t, 4H), 1.6 (m, 4H), 1.3–1.4 (br, 12H), 0.9 (t, 6H).

Polymer **3bd**:  $M_n = 16\,000$  g/mol (SEC); PDI = 4.0.  $^1\text{H}$  NMR (300 MHz,  $\text{CDCl}_3$ ),  $\delta$  (ppm): 7.3 (d, 2H), 7.2 (d, 2H), 7.1 (s, 2H), 7.0 (s, 2H), 4.0 (t, 4H), 1.9 (t, 4H), 1.6 (m, 4H), 1.3–1.4 (br, 8H), 0.9 (t, 6H).

Polymer **3cd**:  $M_n = 22\,000$  g/mol (SEC); PDI = 2.7.  $^1\text{H}$  NMR (300 MHz,  $\text{CDCl}_3$ ),  $\delta$  (ppm): 7.4 (d, 2H), 7.1 (d, 2H), 7.0 (s, 2H), 6.4 (s, 2H), 4.1 (t, 4H), 1.9 (t, 4H), 1.6 (m, 4H), 1.3–1.4 (br, 8H), 0.9 (t, 6H).

Polymer **3ce**:  $M_n = 13\,000$  g/mol (SEC); PDI = 2.3.  $^1\text{H}$  NMR (300 MHz,  $\text{CDCl}_3$ ),  $\delta$  (ppm): 7.4 (d, 2H), 7.1 (d, 2H), 7.0 (s, 2H), 6.4 (s, 2H), 4.1 (t, 4H), 1.9 (t, 4H), 1.6 (m, 4H), 1.3–1.4 (br, 8H), 0.9 (t, 6H).

**Device Characterization.** The field-effect mobilities of poly(phenylene–thiophene–vinylene)s-based TFTs were measured using a top-contact TFT geometry. First, molybdenum (Mo), as a gate electrode, was deposited onto an as-washed glass substrate to a thickness of 2000 Å by a sputtering process, and then a silicon-based organic insulating layer was spun onto the gate electrode to a thickness of 7000 Å ( $C_i = 5.1$  nF/cm<sup>2</sup>). Finally, poly(phenylene–thiophene–vinylene)s were dissolved in chlorobenzene, and then spin-coated on the substrates described above. Source and drain (S/D) electrodes were formed by evaporation of Au (70 nm) using shadow mask. Subsequently, the OTFT devices were annealed at 70 °C for 30 min under N<sub>2</sub>. The standard channel length ( $L$ ) and width ( $W$ ) are 100 and 1000  $\mu\text{m}$ , respectively. All the measurement results were obtained at room temperature in ambient conditions using Keithley 4200 source/measure units.

**Acknowledgment.** Authors thank the Toray Company in Japan for the generous supply of SWCNT solution. Generous financial support from the Korea Research Fund (20090069339 and 20090077075) and BK21 is gratefully acknowledged.

**Supporting Information Available:** Figures showing NMR spectral data, DSC, and UV spectra. This material is available free of charge via the Internet at <http://pubs.acs.org>.

## References and Notes

- (1) Bao, Z.; Locklin, J. *Organic field-effect transistor*; CRC Press: Boca Raton, FL, 2007.
- (2) (a) Klauk, H. *Organic Electronics: Material, Manufacturing, and Applications*; Wiley-VCH: New York, 2006. (b) Sirringhaus, H.; Tessler, N.; Friend, R. H. *Science* **1998**, *281*, 1741.
- (3) (a) Briseno, A. L.; Tseng, R. J.; Ling, M.-M.; Falcao, E. H. L.; Yang, Y.; Wudl, F.; Bao, Z. *Adv. Mater.* **2006**, *18*, 2320. (b) Murphy, A. R.; Fréchet, J. M. J. *Chem. Rev.* **2007**, *107*, 1066.
- (4) Bao, Z.; Dodabalapur, A.; Lovinger, A. J. *Appl. Phys. Lett.* **1996**, *69*, 4108.
- (5) Sirringhaus, H.; Kawase, T.; Friend, R. H.; Shimoda, T.; Inbasekaran, M.; Wu, W.; Woo, E. P. *Science* **2000**, *290*, 2123.
- (6) Ong, B. S.; Wu, Y.; Liu, P.; Gardner, S. J. *Am. Chem. Soc.* **2004**, *126*, 3373.
- (7) McCulloch, I.; Heeney, M.; Bailey, C.; Genevicius, K.; Macdonald, I.; Shkunov, M.; Sparrowe, D.; Tierney, S.; Wagner, R.; Zhang, W.; Chabinyc, M. L.; Kline, R. J.; McGehee, M. D.; Toney, M. F. *Nat. Mat.* **2006**, *5*, 328. (b) For other recent examples, see: Kim, D. W.; Lee, B.-L.; Moon, H.; Kang, H. M.; Jeong, E.-J.; Park, J.-I.; Han, K.-M.; Lee, S.; Yoo, B. W.; Koo, B. W.; Kim, J. Y.; Lee, W. H.; Cho, K.; Becerril, H. A.; Bao, Z. *J. Am. Chem. Soc.* **2009**, *131*, 6124.
- (8) Veres, J.; Ogier, S.; Lloyd, G.; de Leeuw, D. M. *Chem. Mater.* **2004**, *16*, 4543.
- (9) Van Breemen, A. J. J. M.; Herwig, P. T.; Chlon, C. H. T.; Sweetssen, J.; Schoo, H. F. M.; Benito, E. M.; De Leeuw, D. M.; Tanase, C.; Wildeman, J.; Blom, P. W. M. *Adv. Funct. Mater.* **2005**, *15*, 872.
- (10) Chung, D. S.; Lee, S. J.; Park, J. W.; Choi, D. B.; Lee, D. H.; Park, J. W.; Shin, S. C.; Kim, Y. H.; Kwon, S. K.; Park, C. E. *Chem. Mater.* **2008**, *20*, 3450.
- (11) For previous synthesis of the polymers, see the following. (a) Wittig reaction: Saito, H.; Ukai, S.; Iwatshiki, S.; Itoh, T.; Kubo, M. *Macromolecules* **1995**, *28*, 8363. (b) Heck reaction: Okawa, H.; Wada, T.; Sasabe, H. *Synth. Met.* **1997**, *84*, 265.
- (12) Lawrence, N. J.; Muhammad, F. *Tetrahedron* **1998**, *54*, 15361.
- (13) Hou, J.; Yang, C.; Qiao, J.; Li, Y. *Synth. Met.* **2005**, *150*, 297.
- (14) Loewe, R. S.; McCullough, R. D. *Chem. Mater.* **2000**, *12*, 3214.
- (15) Chen, T.-I.; Wu, X.; Rieke, R. D. *J. Am. Chem. Soc.* **1995**, *117*, 233.
- (16) (a) Bao, Z.; Kucj, V.; Rogers, J. A.; Paczkowski, M. A. *Adv. Funct. Mater.* **2002**, *12*, 526. (b) Liu, P.; Wu, Y.; Li, Y.; Ong, B. S.; Zhu, S. J. *Am. Chem. Soc.* **2006**, *128*, 4554.
- (17) (a) Lee, H. S.; Kim, D. H.; Cho, J. H.; Hwang, M.; Jang, Y.; Cho, K. *J. Am. Chem. Soc.* **2008**, *130*, 10556. (b) Ito, Y.; Virkar, A. A.; Mannsfeld, S.; Oh, J. H.; Toney, M.; Locklin, J.; Bao, Z. *J. Am. Chem. Soc.* **2009**, *131*, 9396.
- (18) Kline, R. J.; McGehee, M. D.; Kadnikova, E. N.; Liu, J. S.; Fréchet, J. M. J. *Adv. Mater.* **2003**, *15*, 1519.
- (19) Tsukamoto, J.; Mata, J.; Matsuno, T. *Jpn. J. Appl. Phys.* **2007**, *46*, L396.
- (20) Bo, X. -Z.; Lee, Y.; Strano, M. S.; Goldfinger, M.; Nuckolls, C.; Blanchet, G. B. *Appl. Phys. Lett.* **2005**, *86*, 182102.